Estimating optical lattice alignment by RF spectroscopy

Wei Xiong (熊 炜)[1], Yin Zhang (张 胤)[1], Zhaoyuan Ma (马兆远)[2], and Xuzong Chen (陈徐宗)[1,3*]

[1]*School of Electronics Engineering and Computer Science, Peking University, Beijing 100871, China*

[2]*Shanghai Institute of Optics and Fine Mechanics, Chinese Academy of Science, Shanghai 201800, China*

[3]*State Key Laboratory of Precision Spectroscopy, East China Normal University, Shanghai 200062, China*

[*]*Corresponding author: xuzongchen@pku.edu.cn*

Received March 24, 2012; accepted May 17, 2012; posted online July 13, 2012

A method that uses radio frequency (RF) spectroscopy to evaluate the alignment of an optical lattice is proposed and demonstrated. A one-dimensional (1D) optical lattice is applied along the long axis of a cigar-shaped Bose-Einstein condensate (BEC) in a magnetic trap. The RF spectra of condensates with and without the optical lattice are analyzed, measured, and compared with the condition in which the lattice is misaligned with the BEC. The proposed method greatly optimizes the optical alignments of the lattices.

OCIS codes: 020.1475, 020.7490, 300.6370.

doi: 10.3788/COL201210.090201.

In the field of ultra-cold atoms, the use of optical lattices has drawn increasing interest due to its applications in condense matter physics. Lower temperatures can also be achieved using optical lattices[1−3]. Bose-Einstein condensate (BEC) observations in optical lattices have made the experimental study of matter waves in periodic potentials possible[4−10]. Fundamental studies involve Kapitza-Dirac scattering, Josephson junction dynamics, super fluidity to Mott insulator transitions, number-squeezing, and Bloch oscillations. Ultra-cold atoms in optical lattices also serve as better samples for precision measurements, such as interferometers[11,12] and atomic clocks[13−15].

Apart from the advantages mentioned above, optical lattices offer more control freedom in the experiments. The spatial periodicity of a lattice can be modified by choosing the lattice light wavelength and the angle between the incident laser beams. The lattice depth is adjusted using the light intensity, after which the manifold temporal patterns are obtained using external modulation. Although the aforementioned parameters are controlled with high precision, optical alignment is a problem for lattice experiments. Specifically, imperfect optical alignment with the atomic cloud excites the BEC, thus leading to instabilities. In the conventional method, resonant light from an optical fiber is used as a guide to enable the lattice light to scatter most atoms from the cloud while consuming minimal power. Given that lattice light has a Gaussian profile, the conventional method is less sensitive when the atomic cloud is near the center of the laser beam where the intensity gradient is minimal.

In this letter, we propose a method that uses a radio frequency (RF) field on condensates. We compare the RF spectra of condensates in magnetic traps with and without optical lattices. When the condensates are in the magnetic trap, the RF spectra are influenced by the position-dependent Zeeman shift. Although the optical lattice slightly affects the atomic transition frequency, the misalignment between the center of the magnetic trap and the center of the lattice beam greatly affects the spatial distribution of the atomic cloud, thereby leading to considerable RF spectra variations. Based on RF spectra measurements, we quantify the misalignment and provide precise guidelines to optimize the alignment.

We first considered a $^{87}Rb5^2S_{1/2}\,|F=2,M_F=2\rangle$ condensate in a magnetic trap. It is expressed as a three-dimensional (3D) harmonic trap $U_{\rm M}=U_0+\frac{1}{2}m\omega_{\rm r}^2r^2+\frac{1}{2}m\omega_{\rm z}^2z^2$, where m is the atomic mass, U_0 is the potential bias, $\omega_{\rm r}$ is the radial frequency, r is the radial coordinate, ω_z is the axial frequency, and z is the axial coordinate.

When a red-detuned optical lattice is loaded on the condensate along the axial direction (Fig. 1(a)), the center of the light waist of the lattice $O_{\rm L}$ is assumed to

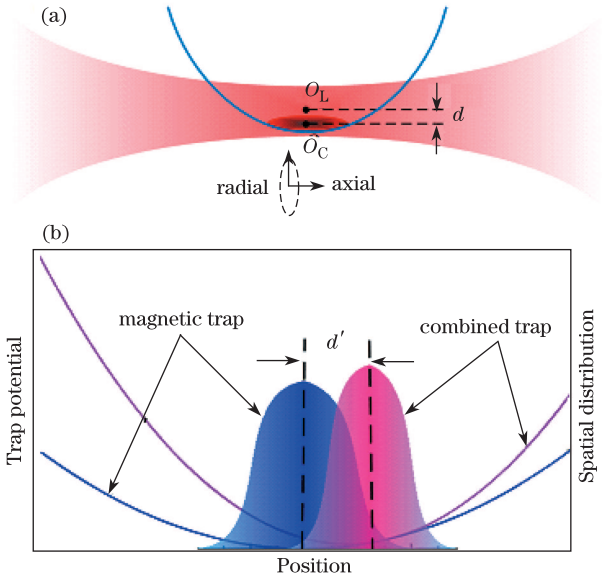

Fig. 1. (Color online) The influence of a misaligned optical lattice on an atomic cloud. (a) A cigar-shaped condensate is loaded in a 1D optical lattice with a displacement d between the center of the condensate $O_{\rm C}$ and the center of the laser beam $O_{\rm L}$ along an arbitrary direction in the radial plane; (b) the spatial distribution of an atomic cloud modified by the optical lattice. Along the direction of d, the atomic cloud in

the combined trap is more compressed and is shifted by d' from the atomic cloud of the magnetic trap.

perfectly overlap with the center of the atomic cloud O_C. However, the assumption is not always true. A displacement d exists between the two centers along an arbitrary direction in the radial plane. Therefore, the trap potential is modified as

$$U_{ML} = U_0 + \frac{1}{2}m\omega_r^2 r^2 + \frac{1}{2}m\omega_z^2 z^2 - U_L \cos^2(k_L z)\left(\frac{w_0}{w_z}\right)^2 \exp\left[\frac{-2(r-d)^2}{w_z^2}\right], \quad (1)$$

where U_L is the lattice depth, k_L is the wave vector, w_0 is the waist size, and w_z is the 1/e radius of the lattice laser. The axial size of condensate is approximately 100 μm, the Rayleigh length of the lattice laser is approximately 5.32×10^4 μm (the Rayleigh length is defined as $Z_R = \pi w_0^2/\lambda_L$, where w_0 is 110 μm and the wavelength of the lattice laser λ_L is 850 nm). The Rayleigh length is over 500 times greater than the typical dimensions of condensates; hence, $w_z \approx w_0$. Given that the lattice was loaded adiabatically, we assumed that the atoms experienced the maximum light intensity along the axial direction. While the radial coordinate r was around d, the potential induced by optical lattice was approximated as a harmonic oscillator trap with frequency ω_L.

The total trap potential is simplified as

$$U_{ML} = U_0 + \frac{1}{6}m\omega_z^2 R_Z^2 - U_L + \frac{1}{2}m\frac{\omega_r^2\omega_L^2}{\omega_r^2+\omega_L^2}d^2 + \frac{1}{2}m(\omega_r^2+\omega_L^2)\left(r - \frac{\omega_L^2}{\omega_r^2+\omega_L^2}d\right)^2, \quad (2)$$

where R_Z is the Thomas Fermi radius along the axial direction. The first line in Eq. (2) represents the bias field of the total potential, whereas the second line is a new harmonic oscillator trap with a higher frequency $\sqrt{\omega_r^2+\omega_L^2}$, and a trap center displacement $d' = \frac{\omega_L^2}{\omega_r^2+\omega_L^2}d$. The atomic cloud is shifted and compressed in space by the new trap (Fig. 1(b)), in which the blue and purple curves are the original and modified traps as well as the spatial distributions, respectively.

For radio frequency (RF) spectroscopy, we used magnetic dipole transitions between the magnetic sub-levels of the hyperfine ground states. The prepared condensate is in the $5^2S_{1/2}|F=2, M_F=2\rangle$ state. Therefore, only one magnetic dipole transition channel, $|F=2, M_F=2\rangle \rightarrow |F'=1, M_F'=1\rangle$, exists between the two hyperfine ground states. For the condensates in the magnetic trap, the frequency shift of the transition from $|F=2, M_F=0\rangle \rightarrow |F'=1, M_F'=0\rangle$ (with a clock transition frequency of 6 834 683 kHz) is mainly influenced by the Zeeman shift (Fig. 2). The atomic cloud is spatially distributed around the center of magnetic trap with a bias B_0. Therefore, the center of the spectra corresponds with the Zeeman shift induced by B_0. This is defined as $(\mu_B g_F M_F B_0 - \mu_B g_{F'} M_F' B_0)/h = 3\mu_B B_0/2h$, where h is the Plank constant, μ_B is the Bohr magneton, $g_F = 1/2$, $M_F = 2$, $g_{F'} = -1/2$, and $M_F' = 1$. The spectra center of the condensates in a magnetic trap is given by $\nu_0 = 6\ 834\ 683$ kHz$+3\mu_B B_0/2h$. When an optical lattice is applied, the center is shifted to $\nu_L = \nu_0 + m\omega_r^2 d'^2/4h$. Both the magnetic field and the lattice light shift the transition based on Eq. (2). We evaluated the frequency shift introduced by the lattice laser based on the methods presented in Refs. [16,17]. The shift has a magnitude of 0.1 Hz, which is negligible compared with the shift caused by the position. The interaction between atoms also causes frequency shifts in condensates. Previous studies have shown that the s-wave scattering lengths of ^{87}Rb in different hyperfine ground states are close to each other[18,19]. Therefore, the collision shift is also negligible.

Meanwhile, the widths of the RF spectra may decrease if the optical lattice loading process is adiabatic. The condensates are adiabatically loaded along the direction of the lattice when the ramping-up time of the lattice loading t_r satisfies $t_r \gg hU_L/16E_R^2 \approx 160$ μs (E_R represents the single photon recoil energy) and $t_r \gg t_I \approx 500$ μs[20], with the characteristic time of mean-field energy t_I. The first condition indicates that the lattice loading is slow enough, thus no atoms are excited to the excitable states. The second condition indicates that the intensity ramp of atomic gas is adiabatic[21]. In our experiment, t_r is 40 ms and meets the two conditions. The adiabaticity of the lattice loading has been demonstrated in Ref. [22]. However, the rising time of the lattice (i.e., 40 ms), and the lattice having a characteristic frequency of 25 Hz might not have been long enough for the optical trap along the radial direction. This is because the frequency gap of the radial harmonic trap is 200 Hz. The loading process causes the excitation and expansion of atomic clouds, thus resulting in the broader width of the RF spectra.

We performed the experiments using an ^{87}Rb BEC system[23,24]. After pre-cooling, a cigar-shaped condensate with 1×10^5 atoms in the $5^2S_{1/2}|F=2\,M_F=2\rangle$ state was obtained by evaporative cooling in a magnetic trap with an axial frequency of 20 Hz and a radial frequency of 200 Hz. The initial atomic gas was prepared as a condensate with negligible hot atoms. A one-dimensional 1D far-red-detuned (wavelength=850 nm) optical lattice was used on the condensate along the axial direction. The lattice depth was $10E_R$, which was

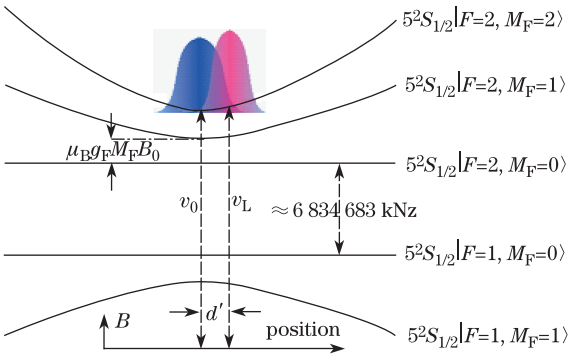

Fig. 2. (Color online) Magnetic sub-levels of the hyperfine ground states of ^{87}Rb in the magnetic trap and the magnetic dipole transition used for RF spectroscopy. A condensate is prepared in the $5^2S_{1/2}|F=2, M_F=2\rangle$ state. Only one channel of the magnetic dipole transition exists for this state and is given by $|F=2, M_F=2\rangle \rightarrow |F=1, M_F=1\rangle$. The transi-

tion in the magnetic trap is shifted from the clock transition by the bias field B_0. The transition in the combined trap is additionally shifted by the displacement d'.

calibrated using Kapitza-Dirac scattering[25]. Evaporation was stopped when the condensates were obtained. The amplitude of the optical lattice increased exponentially after 40 ms and remained constant for another 900 ms (Fig. 3(a)). The RF field was turned on during the same period. The RF field was generated by an arbitrary function generator. It was locked to a high-stability crystal oscillator and coupled out from a horn antenna. The magnetic trap, the optical lattice, and the RF field were turned off at after RF spectroscopy. After 30 ms of free fall, pictures of the atomic gas were taken using absorption imaging in order to measure the number of atoms.

Figure 3(b) shows the schematic of the optical alignment of the lattice. A 780-nm laser was coupled to the same single-mode-polarization-maintaining (SMPM) optical fiber as the lattice laser (850 nm). The resonant light (780 nm) acted as a pilot (without the 0° reflector), which had better alignment and scattered more atoms. We spatially scanned the light alignment until no atoms were left. We then decreased the light power and scanned the light again. We repeated the process until some atoms were observed. Next, we found the right direction that had the lowest number of atoms. The precision of manually aligning the optical lattice was approximately 20 μm per step. In our experiment, we were unable to distinguish the three subsequent steps with the lowest number of observable atoms. Therefore, the actual precision of manual lattice alignment is approximately 60 μm. The radius of lattice light waist is 110 μm, and the precision corresponds to a maximum light instability of 13.8%, which coincides with the fluctuations of approximately 10%. From Eq. (2), the introduced displacement d' is less than 1.3 μm.

The frequency of the RF field was scanned at a fixed power. A frequency range was found in which no $|F = 2, M_F = 2\rangle$ atoms were left. Next, we reduced the RF power, scanned the frequency again, and found a narrower range. We repeated the process until the frequency range reached its minimum. From these steps, we eventually determined the frequency of accurate resonance. When the lattice is turned off, the measured resonant frequency is $\nu_0 = 6\ 838\ 380$ kHz (square dots in Fig. 4(a)). The shift between the frequency and the clock transition is 3 697 kHz. We also obtained the shift using evaporative cooling, which is a good method to read the bias of magnetic traps if evaporation is maintained until no atoms are observed. The final evaporation frequency from evaporative cooling corresponds to $\mu_B B_0/2$ and is approximately 1 191 kHz. The transition shift of approximately $3\mu_B B_0/2 = 3\ 573$ kHz coincides with the results of the RF spectroscopy at a deviation of less than 4%. Deviation may have occurred due to the evaporation system, because the function generator for evaporation is not locked to the high stability crystal oscillator.

Meanwhile, the Thomas-Fermi approximation[26] can be applied to condensates in the harmonic trap. The density distribution is expressed as $\left(1 - \frac{r^2}{R_r^2} - \frac{z^2}{R_Z^2}\right)$, with a radial radius R_r and an axial radius R_Z. The spectra in our experiment reflect different densities at different frequencies, which are related to the position. At the center of the atomic cloud, the density reaches the maximum value and corresponds to the valley on the spectra. The relative population increases slowly from the valley to -4 kHz, and then increases rapidly to nearly the maximum at -5 kHz (square and blue dots in Fig. 4(a)). If the center of the atomic cloud is at the bias field B_0, the rapid increase normally occurs at 0 kHz. However, the spectra behave differently because of gravity. To balance the gravity, the atomic cloud makes a displacement d_g along the direction of gravity in the radial plane from the center of the magnetic field. This satisfies $\frac{d(m\omega_r^2 r_g^2)}{dr_g}\Big|_{r_g=d_g} = mg$, where r_g is along the direction of gravity. The valley matches the position of balance with displacement d_g from the center of the magnetic trap. In our experiment, the displacement d_g is 6.3 μm and causes a shift of 5.1 kHz. The behavior of the spectra on the negative side indicates the behavior of atoms between the balance position and the center of the magnetic trap.

The maximum length of the displacement induced by the optical lattice is 1.3 μm, which is smaller than the 6.3-μm displacement induced by gravity. When the optical lattice is exposed to the atomic cloud in the magnetic trap, a displacement d' is induced, occurring in all directions of the radial plane. The displacement induced by gravity is along a fixed direction, i.e., the y direction. The two vectors composted one d_c with a length that varies from a minimum of $d_g - d'$ to a maximum of $d_g + d'$. The frequency shift of the valley compared with the original varies from -1.9 to 2.3 kHz, corresponding to the minimum and maximum lengths of the composed displacement, respectively. The round dots in Fig. 4(a) are the spectra of the condensates in the magnetic trap and the optical lattice. The valley is shifted approximately $\Delta\nu = -1$ kHz from the condensates in the magnetic trap.

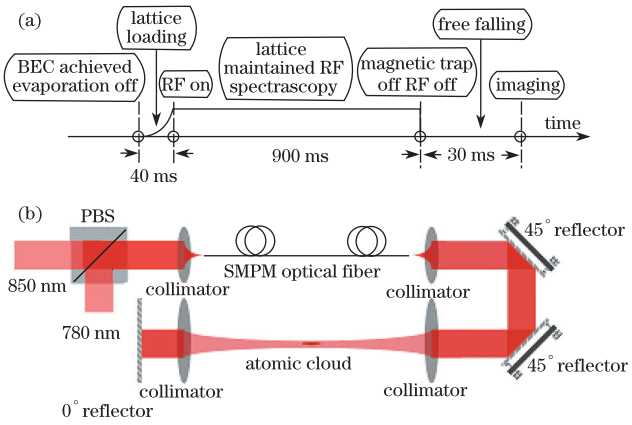

Fig. 3. (Color online) RF spectroscopy of the condensate in the magnetic trap and the optical lattice. (a) The time sequence of the RF spectroscopy. Once a condensate is obtained, the evaporative cooling field is turned off and a 1D optical lattice is ramped exponentially to $10E_R$ after 40 ms. Afterwards, the lattice is maintained at 900 ms, and RF spectroscopy remains turned on at the same time. The lattice, magnetic trap, and RF field are turned off, and TOF signals are taken; (b) Schematic of the optical alignment for the lattice. The lattice light (850 nm) and the pilot light (780 nm) are adjusted to overlap spatially at a polarizing beam splitter and are coupled into a SMPM optical fiber. Light is focused

on the atomic cloud. Adjusting the alignment of the optical lattice blocks the 0° reflector and the lattice light 0°. When the optical lattice works, only the pilot light is blocked.

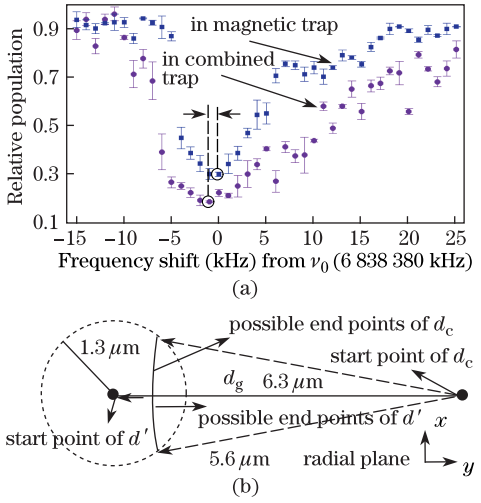

Fig. 4. (Color online) RF spectroscopy of the condensates. (a) Comparison between the spectra of the condensates in the magnetic and combined traps. The square blue dots and the round red dots are the spectra in the magnetic and combined traps, respectively. The valleys encircled in the figure correspond to the centers of the atomic clouds. A frequency shift is also observed ($\Delta\nu = -1$ kHz), which corresponds to the displacement of the atomic gas induced by the optical lattice; (b) evaluation of the 'splacement of atomic gases induced by the optical lattice. The solid line vector d_g is the displacement induced by gravity with a length of 6.3 μm along the negative y direction in the radial plane. The displacement d' is the possible displacement of atomic gases with a length less than 1.3 μm and a direction along any direction in the radial plane. Given that the length of the composed displacement d_c is 5.6 μm, the possible endpoints of d_c and d' are along the 5.6-μm-radius circular arc indicated by the dotted circle.

The length of the composed displacement d_c is obtained as 5.6 μm.

Next, we evaluated the possible lengths and directions of the displacement caused by the optical lattice. The possible vectors of d' came from the starting point to points along the 5.6-μm radius arc within the 1.3-μm radius circle as shown in Fig. 4(b). Then, based on $d' = \frac{\omega_L^2}{\omega_r^2+\omega_L^2} d$, we estimated the misalignment d from the lattice center O_L to the condensate center O_C. If there is a method that allows finer optical adjustment, the lattice alignment is optimized and the overlap of the two centers can be improved further based on RF spectroscopy. When the two centers get closer, the frequency shift between the two spectra becomes smaller. Ideally, if the center of the optical lattice perfectly overlaps with that of the condensate, the shift disappears.

Meanwhile, the positive side of the spectra demonstrates the behavior of atoms beyond the center of the magnetic trap. We evaluate the width of the spectra on the positive side as the shift of the atoms at the half maximum density, and obtain the width about 6.0 kHz.We can read the width as 6.5 kHz on the positive side of the figure, which is reasonable with Doppler and saturation broadening. As the condensates are loaded in the optical lattice, the spectra on the positive side are broadened because of non-adiabatic lattice loading (Fig. 4(a)).

The fluctuations in our experiments are attributed to a number of factors. The first factor is the instability of the initial atom number. Absorption imaging is destructive; thus, we measured the atom number without RF spectroscopy multiple times under the same conditions in order to reduce uncertainty. The average of the measurements was used as the initial atom number. Nevertheless, fluctuations of approximately 5% still occurred. The second factor is the fluctuation of the bias field. We controlled the current of the bias coils at a relative precision of 1×10^{-4}, which corresponds to a transition frequency deviation of approximately 0.36 kHz. The factors limited the precision of the RF spectroscopy.

With the limitations brought about by manual adjustments, we are unable to improve the alignment. Nevertheless, we optimized precision using piezoelectric ceramics for positioning and then scanned the optical alignment using voltages with high precisions of approximately 1 μm. By combining electronic control and RF spectroscopy detection, we aligned the center of the optical lattice O_L closer to the center of the atomic cloud O_C.

If the frequency shift between the two spectra is zero, the lattice alignment is greatly improved. Given that the resolution of the performed spectroscopy is 1 kHz, the actual frequency shift caused by the displacement is within ± 0.5 kHz. This is also within 15 μm of the distance between the two centers O_L and O_C. The precision of the alignment has also been improved from 60 to 15 μm.

In conclusion, we used RF spectroscopy on condensates in magnetic traps with and without optical lattices to reveal the influence of the misalignment of the optical lattice. We analyze the frequency shift of the magnetic dipole transition caused by the magnetic field, gravity, the optical lattice, and the displacement between the center of the optical lattice O_L and the center of the condensate O_C. RF spectra are measured, and experiments and theoretical analysis are then compared. After evaluating the spatial shifts of atomic clouds induced by optical lattices, we find that such shifts are consistent with estimations. Furthermore, better alignment is achieved when the valleys of the two spectra are closer. The proposed method potentially optimizes lattice loading.

This work was supported by the National Fundamental Research Program of China (No. 2011CB921501) and the National Natural Science Foundation of China (Nos. 61027016, 61078026, and 10934010).

References

1. A. Kastberg, W. D. Phillips, S. L. Rolston, and R. J. C. Spreeuw, Phys. Rev. Lett. **74,** 1542 (1995).
2. S. E. Hamann, D. L. Haycock, G. Klose, P. H. Pax, I. H. Deutsch, and P. S. Jessen, Phys. Rev. Lett. **80,** 4149 (1998).
3. H. Perrin, A. Kuhn, I. Bouchoule, and C. Salomon, Europhys. Lett. **42,** 395 (1998).
4. B. P. Anderson and M. A. Kasevich, Science **281,** 1686 (1998).

5. M. Kozuma, L. Deng, E. W. Hagley, J. Wen, R. Lutwak, K. Helmerson, S. L. Rolston, and W. D. Phillips, Phys. Rev. Lett. **82,** 871 (1999).
6. J. Stenger, S. Inouye, A. P. Chikkatur, D. M. Stamper-Kurn, D. E. Pritchard, and W. Ketterle, Phys. Rev. Lett. **82,** 4569 (1999).
7. C. Orzel, A. K. Tuchman, M. L. Fenselau, M. Yasuda, and M. A. Kasevich, Science **291,** 2386 (2001).
8. S. Burger, F. S. Cataliotti, C. Fort, F. Minardi, and M. Inguscio, Phys. Rev. Lett. **86,** 4447(2001).
9. F. S. Cataliotti, S. Burger, C. Fort, P. Maddaloni, F. Minardi, A. Trombettoni, A. Smerzi, and M. Inguscio, Science **293,** 843 (2001).
10. O. Morsch, J. H. Müller, M. Cristiani, D. Ciampini, and E. Arimondo, Phys. Rev. Lett. **87,** 140402 (2001).
11. R. E. Sapiro, R. Zhang, and G. Raithel, Phys. Rev. A **79,** 043630 (2009).
12. S. Beattie1, B. Barrett, I. Chan1, C. Mok, I. Yavin, and A. Kumarakrishnan, Phys. Rev. A **80,** 013618 (2009).
13. M. Takamoto1, F. Hong, R. Higashi, and H. Katori, Nature **435,** 321 (2005).
14. R. Le Targat, X. Baillard, M. Fouché, A. Brusch, O. Tcherbakoff, G. D. Rovera, and P. Lemonde, Phys. Rev. Lett. **97,** 130801 (2006).
15. A. D. Ludlow, T. Zelevinsky, G. K. Campbell, S. Blatt, M. M. Boyd, M. H. G. de Miranda, M. J. Martin, J. W. Thomsen, S. M. Foreman, Jun Ye, T. M. Fortier, J. E. Stalnaker, S. A. Diddams, Y. Le Coq, Z. W. Barber, N. Poli, N. D. Lemke, K. M. Beck, and C. W. Oates, Science **319,** 5871 (2008).
16. X. Zhou, X. Chen, J. Chen, Y. Wang, and J. Li, Chin. Phys. Lett. **26,** 9 (2009).
17. P. Rosenbusch, S. Ghezali, V. A. Dzuba, V. V. Flambaum, K. Beloy, and A. Derevianko, Phys. Rev. A **79,** 013404 (2009).
18. J. L. Roberts, N. R. Claussen, James P. Burke, Jr., Chris H. Greene, E. A. Cornell, and C. E. Wieman, Phys. Rev. Lett. **81,** 5109 (1998).
19. S. L. Cornish, N. R. Claussen, J. L. Roberts, E. A. Cornell, and C. E. Wieman, Phys. Rev. Lett. **85,** 1795 (2000).
20. J. HeckerDenschlag, J. E. Simsarian, H. Häffner, C. McKenzie, A. Browaeys, D. Cho, K. Helmerson, S. L. Rolston, and W. D. Phillips, J. Phys. B **35,** 3095 (2002).
21. C. Orzel, A. K. Tuchman, M. L. Fenselau, M. Yasuda, and M. A. Kasevich, Science **291,** 2386 (2001).
22. B. Lu, T. Vogt, X. Liu, X. Zhou, and X. Chen, Chin. Opt. Lett. **9,** 091403 (2011).
23. X. Zhou, F. Yang, X. Yue, T. Vogt, and X. Chen, Phys. Rev. A **81,** 013615 (2010).
24. B. Lu, T. Vogt, X. Liu, X. Xiao, J. Zhou, and X. Chen, Phys. Rev. A **83,** 051608(R) (2011).
25. R. Sapiro, R. Zhang, and G. Raithel, New J. Phys. **11,** 013013 (2009).
26. W. C. Wu and A. Griffn, Phys. Rev. A **54,** 4204 (1996).